

# Insight into the nature of the $P_c(4457)$ and related pentaquarks

Ulaş Özdem<sup>1, \*</sup>

<sup>1</sup>*Health Services Vocational School of Higher Education,  
Istanbul Aydin University, Sefakoy-Kucukcekmece, 34295 Istanbul, Türkiye*

We systematically study the electromagnetic properties of pentaquark states from different perspectives to better understand their nature, internal structure, and quantum numbers, determine their hadronization processes, and shed light on their true nature. The present study examines the magnetic moments of the  $P_c(4457)$  and related hidden-charm pentaquark states with and without strangeness ( $[dd][uc]\bar{c}$ ,  $[uu][sc]\bar{c}$ ,  $[dd][sc]\bar{c}$ ,  $[ss][uc]\bar{c}$  and  $[ss][dc]\bar{c}$ ), employing a comprehensive analysis that encompasses both the compact pentaquark configuration and  $J^P = \frac{3}{2}^-$  quantum numbers. The present study compares the results regarding the magnetic moment of the  $P_c(4457)$  pentaquark state with those reported in the existing literature. The numerical results obtained in this study, when considered alongside existing literature, indicate that the magnetic moments of hidden-charm pentaquark states may offer insights into their underlying structures, which in turn can inform the distinction between their spin-parity quantum numbers. It seems that for the future experimental search of the family of hidden-charm pentaquark states, studying the electromagnetic properties of the hidden-charm pentaquark states can provide valuable information.

## I. INTRODUCTION

The investigation of exotic states, such as tetraquarks, hybrids, glueballs, and pentaquarks, has become a prominent area of focus in hadron physics following the proposal of the quark model. Given that neither the quark model nor QCD prohibited their existence, these states attracted attention from the outset and were subjected to extensive investigation over an extended period. Ultimately, expectations were fulfilled with the announcement of the first discovery of such states in 2003, namely a tetraquark state,  $X(3872)$ , by the Belle Collaboration. Subsequently, the number of observed exotic states increased and their diversity expanded, following the findings yielded by the aforementioned experimental discovery. A thorough investigation of these exotic states may yield substantial insights into the fundamental processes underlying the dynamics of strong interactions at low energies. In 2015, a novel member of the exotic states, namely the pentaquark state comprising five valence quarks, was reported to have been discovered by the LHCb Collaboration. The two states, designated as  $P_c(4380)$  and  $P_c(4450)$ , were confirmed through observation in the  $J/\psi + p$  decay channel. In 2019, the analyses with a larger data sample yielded further insights. It was revealed that the previously reported  $P_c(4450)$  state had split into  $P_c(4440)$  and  $P_c(4457)$  states, and another pick,  $P_c(4312)^+$ , had also come into sight. It should be noted that the pentaquark  $P_c(4380)$  reported in the previous analysis remains unresolved, neither confirmed nor refuted, in the subsequent analysis. In 2020, the LHCb Collaboration announced a pentaquark state,  $P_{cs}(4459)$ , in the invariant mass spectrum of  $J/\psi\Lambda$  in the  $\Xi_b^0 \rightarrow J/\psi\Lambda K^-$  decay. The measured mass and width are  $4458.8 \pm 2.7_{-1.1}^{+4.7}$  MeV and  $17.3 \pm 6.5_{-5.7}^{+8.0}$  MeV respectively. Recently, the LHCb collaboration observed a new structure  $P_{cs}(4338)$  in the  $J/\psi\Lambda$  mass distribution in the  $B^- \rightarrow J/\psi\Lambda^- p$  decays. The masses, widths, minimal valence quark contents, and observed channels for these states have been listed in Table I.

TABLE I. Hidden-charm pentaquark states reported by the LHCb Collaboration.

| State                | Mass (MeV)                     | Width (MeV)                   | Content       | Observed channels                        |
|----------------------|--------------------------------|-------------------------------|---------------|--|
| $P_c(4380)^+$ [1]    | $4380 \pm 8 \pm 29$            | $215 \pm 18 \pm 86$           | $uudc\bar{c}$ | $\Lambda_b^0 \rightarrow J/\psi p K^-$   |
| $P_c(4312)^+$ [2]    | $4311.9 \pm 0.7_{-0.6}^{+6.8}$ | $9.8 \pm 2.7_{-4.5}^{+3.7}$   | $uudc\bar{c}$ | $\Lambda_b^0 \rightarrow J/\psi p K^-$   |
| $P_c(4440)^+$ [2]    | $4440.3 \pm 1.3_{-4.7}^{+4.1}$ | $20.6 \pm 4.9_{-10.1}^{+8.7}$ | $uudc\bar{c}$ | $\Lambda_b^0 \rightarrow J/\psi p K^-$   |
| $P_c(4457)^+$ [2]    | $4457.3 \pm 0.6_{-1.7}^{+4.1}$ | $6.4 \pm 2.0_{-1.9}^{+5.7}$   | $uudc\bar{c}$ | $\Lambda_b^0 \rightarrow J/\psi p K^-$   |
| $P_{cs}(4459)^0$ [3] | $4458.8 \pm 2.9_{-1.1}^{+4.7}$ | $17.3 \pm 6.5_{-5.7}^{+8.0}$  | $udsc\bar{c}$ | $\Xi_b^- \rightarrow J/\psi \Lambda K^-$ |
| $P_{cs}(4338)^0$ [4] | $4338.2 \pm 0.7 \pm 0.4$       | $7.0 \pm 1.2 \pm 1.3$         | $udsc\bar{c}$ | $B^- \rightarrow J/\psi \Lambda \bar{p}$ |

\* [ulasozdem@aydin.edu.tr](mailto:ulasozdem@aydin.edu.tr)

Along with the aforementioned hidden-charm pentaquark states, searches for doubly and triply strange hidden-charm pentaquarks are currently underway, with the CMS Collaboration recently observing the decay  $\Lambda_b^0 \rightarrow J/\psi \Xi^- K^+$  [5]. Nevertheless, insufficient yield and inadequate resolution prevented the observation of a clear spectrum in the  $J/\psi \Xi^-$  invariant mass. These results are significant in elucidating the underlying strong interaction processes in the hadronic decays of beauty baryons and the potential mechanism for forming exotic states. The observations in question have generated considerable excitement, leading to the intensified theoretical study of these hadrons. The objective of these theoretical studies was to investigate the properties of these states in order to gain insight into their natures and substructures. Moreover, some of these studies concentrated on the potential for the emergence of additional states, intending to provide insights that could inform future experimental observations. A variety of approaches and structural assumptions were employed to conduct a comprehensive investigation of the observed states [6–21].

Despite the extensive research conducted since the initial observation of these states, our knowledge of their exact nature, internal structure, and quantum numbers remains incomplete. It is thus evident that further investigation into their properties is required. The present study examines the magnetic moments of the  $P_c(4457)$  and related hidden-charm pentaquark states with and without strangeness ( $[dd][uc]\bar{c}$ ,  $[uu][sc]\bar{c}$ ,  $[dd][sc]\bar{c}$ ,  $[ss][uc]\bar{c}$  and  $[ss][dc]\bar{c}$ ), employing a comprehensive analysis that encompasses both the compact pentaquark configuration and  $J^P = \frac{3}{2}^-$  quantum numbers. It is widely acknowledged that magnetic moments represent physical parameters that are directly correlated with the inner structure of the state under investigation. Accordingly, the aforementioned parameters facilitate the extraction of insights concerning the internal structure of the hadron and the low-energy domain of QCD. Furthermore, magnetic moments represent an effective tool for investigating the dynamics of quarks and gluons within a hadron. This is due to the fact that it represents the leading-order response of a bound state to an external magnetic field. Despite the priceless insights they can provide, there are few investigations of the magnetic moments of hidden-charm/bottom pentaquarks in the available literature [22–43]. While the short lifetime of the  $P_c$  states currently presents a significant challenge for measuring the magnetic moment, the accumulation of more extensive data from future experiments may facilitate the achievement of this goal. The  $\Delta^+(1232)$  baryon has also a very short lifetime, however, its magnetic moment was achieved through  $\gamma N \rightarrow \Delta \rightarrow \Delta\gamma \rightarrow \pi N\gamma$  process [44–46]. A comparable process,  $\gamma^{(*)}N \rightarrow P_c \rightarrow P_c\gamma \rightarrow J/\psi N\gamma$ , may be employed to derive the magnetic moment of the  $P_c$  pentaquarks. Moreover, the magnetic moments of baryons containing two charm quarks have been calculated using techniques from lattice QCD [47, 48]. The possibility exists for these analyses to be extended soon to encompass exotic states.

We organize this paper in the following manner: In Sec. II we present the results of a QCD light-cone sum rule analysis within an external background field method, which are conducted to calculate the magnetic moment of the considered states, which we have labeled as  $P_c$ . Additionally, we present an analysis of the results obtained from these analyses. Sec. III is dedicated to a comprehensive numerical analysis of the magnetic moments of the  $P_c$  states. Finally, this work ends with the summary in Sec. IV.

## II. THEORETICAL FORMALISM FOR THE MAGNETIC MOMENT

The QCD light-cone sum rule represents a widely accepted and productive methodology for the determination of the measurable properties of hadrons, including the calculation of their form factors, the analysis of their strong and weak decay properties, and their investigation in the context of radiative decays [49–51]. The fundamental premise of the methodology is the calculation of the correlation function, which constitutes a pivotal element of the methodology. This is accomplished through two distinct approaches: the QCD approach and the hadronic approach. At the hadronic level, hadronic parameters, including residues, masses, and form factors, are utilized. In contrast, at the QCD level, parameters associated with QCD, such as the quark condensate, gluon condensate, and particle distribution amplitudes, among others, are employed. Subsequently, the Borel transformation and continuum subtraction are employed. The aforementioned procedures yield sum rules for the physics parameter to be calculated.

Following a brief introduction to the method, we may now proceed with the analysis of the physical parameter in question using this approach. As previously stated, the initial step is to define the correlation function of interest. The correlation function to be employed in the analysis of the magnetic moment of the  $P_c$  states is provided by the following formula:

$$\Pi_{\mu\nu}(p, q) = i \int d^4x e^{ip \cdot x} \langle 0 | T \{ J_\mu(x) \bar{J}_\nu(0) \} | 0 \rangle_\gamma, \quad (1)$$

where the  $J_\mu(x)$  stands for interpolating current of the  $P_c$  states,  $\gamma$  is the external electromagnetic field, and  $q$  is the momentum of the photon. The relevant expression for the  $J_\mu(x)$  is presented as follows:

$$J_\mu(x) = \frac{\mathcal{A}}{\sqrt{3}} \left\{ [q_{1d}^T(x) C \gamma_\mu q_{1e}(x)] [q_{2f}^T(x) C \gamma_5 c_g(x)] C \bar{c}_c^T(x) + 2 [q_{1d}^T(x) C \gamma_\mu q_{2e}(x)] [q_{1f}^T(x) C \gamma_5 c_g(x)] C \bar{c}_c^T(x) \right\}, \quad (2)$$

where  $\mathcal{A} = \varepsilon_{abc} \varepsilon_{ade} \varepsilon_{bfg}$  with  $a, b, c, d, e, f$  and  $g$  being color indices; and the  $C$  is the charge conjugation operator. The quark content of the  $P_c$  states is listed in Table II.

TABLE II. The quark content of the  $P_c$  states.

| States | $[uu][d\bar{c}]\bar{c}$ | $[d\bar{d}][u\bar{c}]\bar{c}$ | $[uu][s\bar{c}]\bar{c}$ | $[d\bar{d}][s\bar{c}]\bar{c}$ | $[ss][u\bar{c}]\bar{c}$ | $[ss][d\bar{c}]\bar{c}$ |
|--------|-------------------------|-------------------------------|-------------------------|-------------------------------|-------------------------|-------------------------|
| $q_1$  | u                       | d                             | u                       | d                             | s                       | s                       |
| $q_2$  | d                       | u                             | s                       | s                             | u                       | d                       |

In this step of the analysis, we will demonstrate how to derive the magnetic moment calculation in the form of hadronic parameters. In order to achieve this, a complete set with the same quantum numbers as the interpolating currents in Eq. (1) is incorporated into the correlation function. The resulting outcome is as follows:

$$\Pi_{\mu\nu}^{Had}(p, q) = \frac{\langle 0 | J_\mu(x) | P_c(p_2) \rangle \langle P_c(p_2) | P_c(p_1) \rangle_\gamma \langle P_c(p_1) | \bar{J}_\nu(0) | 0 \rangle}{[p_2^2 - m_{P_c}^2] [p_1^2 - m_{P_c}^2]}, \quad (3)$$

where  $p_1 = p + q$ ,  $p_2 = p$ . As can be observed from the provided formulas, matrix elements such as  $\langle 0 | J_\mu(x) | P_c(p_2, s) \rangle$ ,  $\langle P_c(p_1, s) | \bar{J}_\nu^P(0) | 0 \rangle$ , and  $\langle P_c(p_2) | P_c(p_1) \rangle_\gamma$  emerge and are necessary for the remainder of the analysis. The aforementioned expressions are presented in the following manner:

$$\langle 0 | J_\mu(x) | P_c(p_2, s) \rangle = \lambda_{P_c} u_\mu(p_2, s), \quad (4)$$

$$\langle P_c(p_1, s) | \bar{J}_\nu(0) | 0 \rangle = \lambda_{P_c} \bar{u}_\nu(p_1, s), \quad (5)$$

$$\begin{aligned} \langle P_c(p_2) | P_c(p_1) \rangle_\gamma &= -e \bar{u}_\mu(p_2) \left\{ F_1(q^2) g_{\mu\nu} \not{\epsilon} - \frac{1}{2m_{P_c}} \left[ F_2(q^2) g_{\mu\nu} \not{\epsilon} \not{q} + F_4(q^2) \frac{q_\mu q_\nu \not{\epsilon} \not{q}}{(2m_{P_c})^2} \right] \right. \\ &\quad \left. + \frac{F_3(q^2)}{(2m_{P_c})^2} q_\mu q_\nu \not{\epsilon} \right\} u_\nu(p_1), \end{aligned} \quad (6)$$

where  $\lambda_{P_c}$  is current coupling of the  $P_c$  states;  $u_\mu(p_2, s)$  and  $\bar{u}_\nu(p_1, s)$  are the spinors of the  $P_c$  states;  $\varepsilon$  is the photon's polarization vector, and  $F_i(q^2)$  are transition form factors. By employing the Eqs. (3) to (6) and making the requisite simplifications, the expressions for the magnetic moment of the  $P_c$  states in conjunction with hadronic parameters are as follows:

$$\begin{aligned} \Pi_{\mu\nu}^{Had}(p, q) &= -\frac{\lambda_{P_c}^2}{[p_1^2 - m_{P_c}^2][p_2^2 - m_{P_c}^2]} (\not{p}_1 + m_{P_c}) \left[ g_{\mu\nu} - \frac{1}{3} \gamma_\mu \gamma_\nu - \frac{2p_{1\mu} p_{1\nu}}{3m_{P_c}^2} + \frac{p_{1\mu} \gamma_\nu - p_{1\nu} \gamma_\mu}{3m_{P_c}} \right] \left\{ F_1(q^2) g_{\mu\nu} \not{\epsilon} \right. \\ &\quad \left. - \frac{1}{2m_{P_c}} \left[ F_2(q^2) g_{\mu\nu} \not{\epsilon} \not{q} + F_4(q^2) \frac{q_\mu q_\nu \not{\epsilon} \not{q}}{(2m_{P_c})^2} \right] + \frac{F_3(q^2)}{(2m_{P_c})^2} q_\mu q_\nu \not{\epsilon} \right\} (\not{p}_2 + m_{P_c}) \left[ g_{\mu\nu} - \frac{1}{3} \gamma_\mu \gamma_\nu - \frac{2p_{2\mu} p_{2\nu}}{3m_{P_c}^2} \right. \\ &\quad \left. + \frac{p_{2\mu} \gamma_\nu - p_{2\nu} \gamma_\mu}{3m_{P_c}} \right]. \end{aligned} \quad (7)$$

In general, the expression of the desired physical parameters can be achieved through the use of hadronic quantities in accordance with the previously established Eq. (7). However, at this juncture, an additional step can be taken to further enhance the reliability and consistency of the analytical procedure. In the expressions of Eq. (7), both spin-1/2 hadrons contribute, and not all Lorentz structures are independent. In order to define the matrix element of the vacuum and the interpolating current between the spin-1/2 hadrons, it is possible to proceed as follows:

$$\langle 0 | J_\mu(0) | H(p, s = 1/2) \rangle = (A p_\mu + B \gamma_\mu) u(p, s = 1/2). \quad (8)$$

As demonstrated by the equation, the undesired effects associated with spin-1/2 hadrons have been found to be proportional to both  $\gamma_\mu$  and  $p_\mu$ . In order to remove the undesired contamination from the spin-1/2 hadrons and to obtain a correlation function comprising solely independent structures, we have devised the following ordering of the Dirac matrices:  $\gamma_\mu \not{p} \not{\epsilon} \not{q} \gamma_\nu$ . Subsequently, in order to guarantee the exclusion of these irrelevant elements

from the analysis, it is necessary to eliminate any terms with  $\gamma_\mu$  at the beginning and  $\gamma_\nu$  at the end, or that are directly proportional to  $p_{2\mu}$  or  $p_{1\nu}$  [52]. The outcome of the examination conducted at the hadron level, after the implementation of the aforementioned procedures, is presented in the following form:

$$\begin{aligned} \Pi_{\mu\nu}^{Had}(p, q) &= \frac{\lambda_{P_c}^2}{[(p+q)^2 - m_{P_c}^2][p^2 - m_{P_c}^2]} \left[ g_{\mu\nu} \not{p} \not{q} F_1(q^2) - m_{P_c} g_{\mu\nu} \not{q} F_2(q^2) - \frac{F_3(q^2)}{4m_{P_c}} q_\mu q_\nu \not{q} \right. \\ &\quad \left. - \frac{F_4(q^2)}{4m_{P_c}^3} (\varepsilon \cdot p) q_\mu q_\nu \not{p} \not{q} + \text{other independent structures} \right]. \end{aligned} \quad (9)$$

It may be more meaningful to express the form factors given in Eq. (9) regarding the magnetic form factor, denoted as  $G_M(q^2)$ , given that this is an experimentally accessible quantity. The expression for this is provided below [53–56]:

$$G_M(q^2) = [F_1(q^2) + F_2(q^2)] \left(1 + \frac{4}{5}\tau\right) - \frac{2}{5} [F_3(q^2) + F_4(q^2)] \tau (1 + \tau), \quad (10)$$

where  $\tau = -\frac{q^2}{4m_{P_c}^2}$ . At  $q^2 = 0$ , the  $G_M(0)$  regarding the  $F_i(0)$  form factors is given by

$$G_M(0) = F_1(0) + F_2(0). \quad (11)$$

Given the focus of our study on the analysis of magnetic moments, it is imperative that the magnetic moment is expressed following the previously mentioned form factors. The magnetic moment, designated as  $(\mu_{P_c})$ , can be derived from the aforementioned term through the following process:

$$\mu_{P_c} = \frac{e}{2m_{P_c}} G_M(0). \quad (12)$$

The calculation of the analysis in connection with the hadronic parameters has now been completed. The next phase of the calculations, conducted at the quark-gluon level, can now commence. To perform this phase of the analysis, the relevant interpolating currents are injected into the correlation function and all the relevant contractions are performed with the help of Wick's theorem. The result of this procedure is as follows:

$$\begin{aligned} \Pi_{\mu\nu}^{QCD}(p, q) &= \frac{i}{3} \mathcal{A} \mathcal{A}' \int d^4x e^{ip \cdot x} \langle 0 | \{ \\ &\quad - \text{Tr} \left[ \gamma_\mu S_{q_1}^{ee'}(x) \gamma_\nu S_{q_1}^{dd'T}(x) C \right] \text{Tr} \left[ \gamma_5 S_c^{gg'}(x) \gamma_5 C S_{q_2}^{ff'T}(x) C \right] \\ &\quad + \text{Tr} \left[ \gamma_\mu S_{q_1}^{ed'}(x) \gamma_\nu C S_{q_1}^{de'T}(x) C \right] \text{Tr} \left[ \gamma_5 S_c^{gg'}(x) \gamma_5 C S_{q_2}^{ff'T}(x) C \right] \\ &\quad + 2 \text{Tr} \left[ \gamma_5 S_c^{gg'}(x) \gamma_5 C S_{q_1}^{ef'T}(x) C \gamma_\mu S_{q_1}^{dd'}(x) \gamma_\nu C S_{q_2}^{fe'T}(x) C \right] \\ &\quad - 2 \text{Tr} \left[ \gamma_5 S_c^{gg'}(x) \gamma_5 C S_{q_1}^{df'T}(x) C \gamma_\mu S_{q_1}^{ed'}(x) \gamma_\nu C S_{q_2}^{fe'T}(x) C \right] \\ &\quad - 4 \text{Tr} \left[ \gamma_\mu S_{q_2}^{ee'}(x) \gamma_\nu S_{q_1}^{dd'T}(x) C \right] \text{Tr} \left[ \gamma_5 S_c^{gg'}(x) \gamma_5 C S_{q_1}^{ff'T}(x) C \right] \\ &\quad + 4 \text{Tr} \left[ \gamma_\mu S_{q_2}^{ee'}(x) \gamma_\nu C S_{q_1}^{fd'T}(x) C \right] \text{Tr} \left[ \gamma_5 S_c^{gg'}(x) \gamma_5 C S_{q_1}^{df'T}(x) C \right] \\ &\quad + 2 \text{Tr} \left[ \gamma_5 S_c^{gg'}(x) \gamma_5 C S_{q_2}^{ef'T}(x) C \gamma_\mu S_{q_1}^{dd'}(x) \gamma_\nu C S_{q_1}^{fe'T}(x) C \right] \\ &\quad \left. - 2 \text{Tr} \left[ \gamma_5 S_c^{gg'}(x) \gamma_5 C S_{q_2}^{ef'T}(x) C \gamma_\mu S_{q_1}^{de'}(x) \gamma_\nu C S_{q_1}^{fd'T}(x) C \right] \right\} \left( C S_c^{cT}(-x) C \right) | 0 \rangle_\gamma, \end{aligned} \quad (13)$$

The  $S_q(x)$  and  $S_c(x)$  in Eq. (13) are the related full quark propagators, which are given as [57, 58]

$$S_q(x) = S_q^{free}(x) - \frac{\langle \bar{q}q \rangle}{12} \left(1 - i \frac{m_q \not{x}}{4}\right) - \frac{\langle \bar{q}q \rangle}{192} m_0^2 x^2 \left(1 - i \frac{m_q \not{x}}{6}\right) + \frac{ig_s G^{\mu\nu}(x)}{32\pi^2 x^2} [\not{x} \sigma_{\mu\nu} + \sigma_{\mu\nu} \not{x}], \quad (14)$$

$$S_c(x) = S_c^{free}(x) - \frac{m_c g_s G^{\mu\nu}(x)}{32\pi^2} \left[ (\sigma_{\mu\nu} \not{x} + \not{x} \sigma_{\mu\nu}) \frac{K_1(m_c \sqrt{-x^2})}{\sqrt{-x^2}} + 2\sigma_{\mu\nu} K_0(m_c \sqrt{-x^2}) \right], \quad (15)$$

with

$$S_q^{free}(x) = \frac{1}{2\pi x^2} \left( i \frac{\not{x}}{x^2} - \frac{m_q}{2} \right), \quad (16)$$

$$S_c^{free}(x) = \frac{m_c^2}{4\pi^2} \left[ \frac{K_1(m_c \sqrt{-x^2})}{\sqrt{-x^2}} + i \frac{\not{x} K_2(m_c \sqrt{-x^2})}{(\sqrt{-x^2})^2} \right]. \quad (17)$$

where  $K_n$  are modified Bessel functions of the second kind. Here, we use the following integral representation of the modified second-type Bessel function,

$$K_n(m_Q \sqrt{-x^2}) = \frac{\Gamma(n+1/2) 2^n}{m_Q^n \sqrt{\pi}} \int_0^\infty dt \cos(m_Q t) \frac{(\sqrt{-x^2})^n}{(t^2 - x^2)^{n+1/2}}. \quad (18)$$

The photon interacts with quarks in two distinct ways: at short distances, which is referred to as the perturbative contribution, and at long distances, which is known as the non-perturbative contribution. The perturbative contributions pertain to the short-distance interaction of the photon with all quark fields. In contrast, the non-perturbative contributions are concerned with the long-distance interaction of the photon with light quark fields.

To account for perturbative contributions in the computations, one of the light or heavy quark propagators that are in interaction with the photon must be modified according to the following substitution:

$$S^{free}(x) \rightarrow \int d^4 z S^{free}(x-z) \not{A}(z) S^{free}(z). \quad (19)$$

To include non-perturbative elements in the computations, it is essential to modify one of the light quark propagators that interact with the photon at a long-distance, in adherence to the following replacement:

$$S_{\alpha\beta}^{ab}(x) \rightarrow -\frac{1}{4} [\bar{q}^a(x) \Gamma_i q^b(0)] (\Gamma_i)_{\alpha\beta}, \quad (20)$$

where  $\Gamma_i = 1, \gamma_5, \gamma_\mu, i\gamma_5\gamma_\mu, \sigma_{\mu\nu}/2$ . In the context of the non-perturbative analysis, the terms  $\langle \gamma(q) | \bar{q}(x) \Gamma_i G_{\mu\nu} q(0) | 0 \rangle$  and  $\langle \gamma(q) | \bar{q}(x) \Gamma_i q(0) | 0 \rangle$  appear and are pivotal to the remainder of the computations. These terms are expressed about the distribution amplitudes of the photon, along with associated parameters, as detailed in Ref. [59]. Since these aspects of the analysis are technical and have been standardized, we have not included further detail here. Those interested in this topic may wish to consult the Refs. [60, 61], which provides more detailed information and a more comprehensive account of the procedures in question. Eqs. (19) and (20) have been employed to incorporate both perturbative and non-perturbative contributions into the analysis, following the established methodology.

Analytical expressions are provided for the magnetic moment of the  $P_c$  states, wherein both hadronic and quark-gluon parameters are given by the formula.

$$\mu_{P_c} \lambda_{P_c}^2 = e \frac{m_{P_c}^2}{M^2} \rho(M^2, s_0). \quad (21)$$

The results for the function  $\rho(M^2, s_0)$  are presented in the appendix.

### III. NUMERICAL ILLUSTRATIONS

This section presents the results of a numerical analysis of the QCD light-cone sum rule, which was conducted in order to make predictions regarding the magnetic moments of the  $P_c$  states. A prerequisite to undertaking the numerical analysis of the QCD light-cone sum rule is to ascertain the numerical values of many parameters. In order to facilitate a comprehensive analysis, a set of values has been adopted for the parameters in question:  $m_s = 93.4_{-3.4}^{+8.6}$  MeV,  $m_c = 1.27 \pm 0.02$  GeV [62],  $m_{P_c(4457)} = 4457.3 \pm 0.6_{-1.7}^{+4.1}$  MeV [63],  $m_{[dd][uc]\bar{c}} = 4.47 \pm 0.11$  GeV [64],  $m_{[uu][sc]\bar{c}} = 4.51 \pm 0.12$  GeV [65],  $m_{[dd][sc]\bar{c}} = 4.51 \pm 0.12$  GeV [65],  $m_{[ss][uc]\bar{c}} = 4.60 \pm 0.11$  GeV [65],  $m_{[ss][dc]\bar{c}} = 4.60 \pm 0.11$  GeV [65],  $\langle \bar{u}u \rangle = \langle \bar{d}d \rangle = (-0.24 \pm 0.01)^3$  GeV<sup>3</sup>,  $\langle \bar{s}s \rangle = 0.8 \langle \bar{u}u \rangle$  GeV<sup>3</sup> [66],  $m_0^2 = 0.8 \pm 0.1$  GeV<sup>2</sup> [66], and  $\langle g_s^2 G^2 \rangle = 0.48 \pm 0.14$  GeV<sup>4</sup> [67]. In addition, we require the residues of the  $P_c$  states, which have been taken from Refs. [64, 65]. In numerical calculations, we fix  $m_u = m_d = 0$  and  $m_s^2 = 0$ , but taking into account terms proportional to  $m_s$ . To perform further computations, it is essential to utilize the photon DAs and their explicit form, together with the necessary numerical values, as outlined in Ref. [59].

In consideration of the previously outlined numerical input variables, two additional parameters are requisite for the implementation of our numerical analysis. These are the continuum threshold parameter, designated as  $s_0$ , and the

Borel parameter, represented by  $M^2$ . In an ideal context, the numerical analysis would be conducted in a manner that is independent of the aforementioned parameters. Nevertheless, this is not a viable approach in practice. It is therefore necessary to establish a region of analysis in which the influence of parameter variation on the numerical results is to be regarded as insignificant. The range of applicability of these parameters is contingent upon the methodology employed, and the variation in numerical results concerning these specified parameters is minimal within the specified interval. The working region for these parameters, which is the interval where the variation in our numerical results for these parameters is small, is subject to the constraints imposed by the methodology used. Such limitations are commonly designated as pole contribution (PC) and convergence of OPE (CVG). The aforementioned constraints are defined following the relevant formulas as follows:

$$\text{PC} = \frac{\rho(M^2, s_0)}{\rho(M^2, \infty)}, \quad (22)$$

$$\text{CVG} = \frac{\rho^{\text{DimN}}(M^2, s_0)}{\rho(M^2, s_0)}, \quad (23)$$

where  $\text{DimN} \geq 10$ . Following the sum rules analysis, the CVG is required to be sufficiently small to ensure the convergence of the OPE, whereas the PC is obliged to be sufficiently large in order to optimize the efficiency of the single-pole approach. The PC and CVG values obtained from the computational analysis are displayed in Table III, along with the designated working intervals of the  $s_0$ , and  $M^2$  for the states under study. To guarantee the dependability of the derived working intervals, we have taken the state of  $P_c(4457)$  as an example, the variations of the calculated magnetic moment values about the specified auxiliary variables are plotted in Fig. 1. As anticipated, the figure illustrates a slight discrepancy in the outcomes observed within these specified intervals. Though the magnetic moments of these states show a slight dependence on these quantities, they remain within the permissible limits of this methodology, representing the primary source of uncertainty.

All requisite parameters for the numerical analysis have been identified and defined. The complete numerical results, inclusive of all inherent variabilities associated with the input parameters, are presented in Table III.

TABLE III. Numerical results of the magnetic moment of the  $P_c$  states together with working intervals of helping parameters.

| State             | $\mu$ [ $\mu_N$ ]       | $s_0$ [ $\text{GeV}^2$ ] | $M^2$ [ $\text{GeV}^2$ ] | CVG [%] | PC [%]       |
|-------------------|-------------------------|--------------------------|--------------------------|---------|--------------|
| $P_c(4457)$       | $-1.96^{+0.50}_{-0.37}$ | [26.0, 28.0]             | [2.6, 3.2]               | 1.92    | [35.1, 57.0] |
| $[dd][uc]\bar{c}$ | $-2.04^{+0.46}_{-0.41}$ | [26.0, 28.0]             | [2.6, 3.2]               | 1.93    | [34.7, 56.9] |
| $[uu][sc]\bar{c}$ | $-2.08^{+0.53}_{-0.39}$ | [27.0, 29.0]             | [2.8, 3.4]               | 1.95    | [33.2, 53.8] |
| $[dd][sc]\bar{c}$ | $-2.13^{+0.53}_{-0.40}$ | [27.0, 29.0]             | [2.8, 3.4]               | 1.94    | [33.5, 54.4] |
| $[ss][uc]\bar{c}$ | $-2.29^{+0.53}_{-0.39}$ | [28.0, 30.0]             | [2.9, 3.5]               | 1.91    | [35.0, 55.2] |
| $[ss][dc]\bar{c}$ | $-2.33^{+0.53}_{-0.41}$ | [28.0, 30.0]             | [2.9, 3.5]               | 1.90    | [35.1, 55.3] |

The findings that are obtained from the numerical results can be interpreted as follows:

- Magnetic moment size can be used to provide insight into the experimental accessibility of such entities. The magnetic moments determined for the hidden-charm pentaquarks are considerably large. The magnitude of these results points to the possibility that they may be achievable in future experiments.
- The results obtained for the magnetic moment are dominated by the charm quark (terms proportional to  $e_c$  (80%) and light-quarks (20%)).
- The  $U$ -symmetry violation in the results is obtained as a maximum of 11%. From these results, one can see that a reasonable  $U$ -symmetry violation is observed.

- To obtain further insight, it would be beneficial to conduct a comparative analysis between the numerical values obtained and the existing literature on the subject. In Ref. [27], the magnetic moment of the  $P_c(4457)$  state was investigated within the framework of the QCD light-cone sum rules for both molecular and compact pentaquark configurations with  $J^P = 1/2^-$  quantum numbers. The resulting values are designated as  $\mu_{P_c(4457)} = 2.78^{+0.94}_{-0.83} \mu_N$  and  $\mu_{P_c(4457)} = 0.88^{+0.32}_{-0.29} \mu_N$  for the molecular and compact pentaquark configurations, respectively. In Ref. [28], the magnetic moment of the  $P_c(4457)$  state was investigated in the quark model with the quantum numbers  $J^P = 3/2^-$ , with and without coupled channel and  $D$ -wave effects. It has been considered that this pentaquarks are in the molecular picture. The resulting value is  $\mu_{P_c(4457)} = (1.145 - 1.365) \mu_N$ . The results exhibit considerable discrepancies, not only in magnitude but also in sign.
- The numerical results obtained in this study, when considered alongside existing literature, indicate that the magnetic moments of hidden-charm pentaquark states may offer insights into their underlying structures, which in turn can inform the distinction between their spin-parity quantum numbers. To get a more conclusive picture of these results, further studies are encouraged.

#### IV. SUMMARY

We systematically study the electromagnetic properties of pentaquark states from different perspectives to better understand their nature, internal structure, and quantum numbers, determine their hadronization processes, and shed light on their true nature. The present study examines the magnetic moments of the  $P_c(4457)$  and related hidden-charm pentaquark states with and without strangeness ( $[dd][uc]\bar{c}$ ,  $[uu][sc]\bar{c}$ ,  $[dd][sc]\bar{c}$ ,  $[ss][uc]\bar{c}$  and  $[ss][dc]\bar{c}$ ), employing a comprehensive analysis that encompasses both the compact pentaquark configuration and  $J^P = \frac{3}{2}^-$  quantum numbers. The present study compares the results regarding the magnetic moment of the  $P_c(4457)$  pentaquark state with those reported in the existing literature. The numerical results obtained in this study, when considered alongside existing literature, indicate that the magnetic moments of hidden-charm pentaquark states may offer insights into their underlying structures, which in turn can inform the distinction between their spin-parity quantum numbers. It seems that for the future experimental search of the family of hidden-charm pentaquark states, the study of the electromagnetic properties of the hidden-charm pentaquark states can provide valuable information. We hope that these revelations will motivate our experimental colleagues to probe further into the family of hidden-charm pentaquark states and to explore the inner structure of  $P_c(4457)$  in future studies.

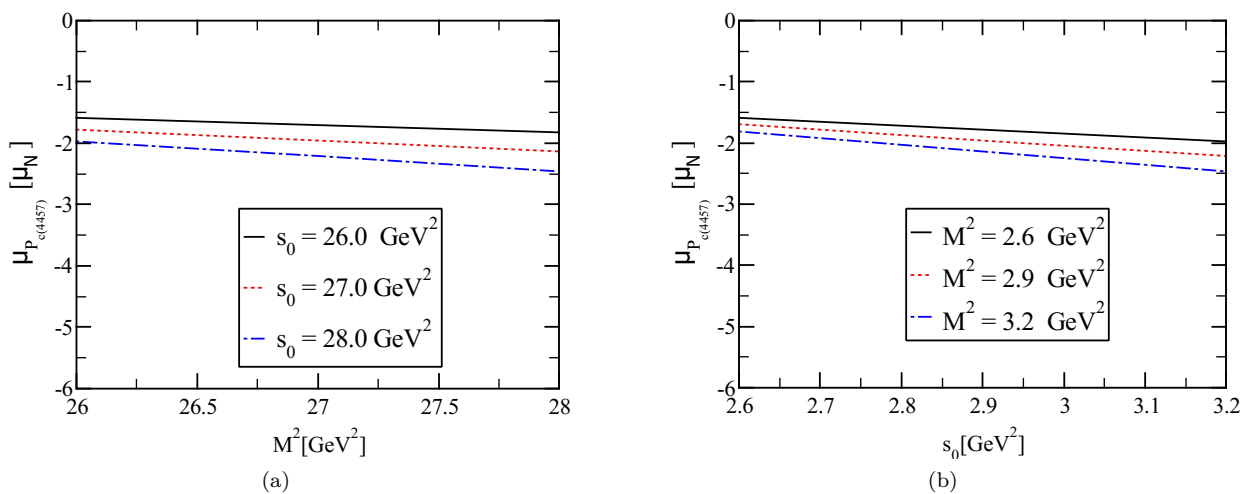


FIG. 1. The magnetic moments of the  $P_c(4457)$  state versus  $M^2$  (left panel) and  $s_0$  (right panel).

**APPENDIX: ANALYTICAL RESULTS FOR  $\rho(M^2, s_0)$  FUNCTIONS**

In this appendix, we present analytical results for the functions  $\rho(M^2, s_0)$ ,

$$\rho(M^2, s_0) = F_1(M^2, s_0) - \frac{1}{m_{P_{cs}}} F_2(M^2, s_0), \quad (24)$$

with

$$\begin{aligned}
F_1(M^2, s_0) = & -\frac{e_c}{2^{25} \times 3^3 \times 5^3 \times 7^2 \times \pi^7} \left( 3752 m_{q_1} m_c I[0, 6] - 855 I[0, 7] \right) \\
& + \frac{C_1 C_2 C_3}{2^{17} \times 3^6 \times 5 \times \pi^3} \left( 45 e_c m_{q_1} m_c I[0, 1] - 11(e_c + e_{q_1}) I[0, 2] \right) \\
& + \frac{C_1 C_2^2}{2^{17} \times 3^5 \times \pi^3} \left( (e_c - 2e_{q_2}) m_{q_1} m_c I[0, 1] \right) \\
& + \frac{C_1 C_2}{2^{22} \times 3^7 \times 5 \times \pi^5} \left( m_0^2 \left( -220(e_{q_1} + e_{q_2}) m_{q_1} - 3(197e_{q_1} + 251e_{q_2}) m_c + e_c(671m_{q_1} + 402m_c) \right) \right. \\
& \times I[0, 2] + \left. \left( -901e_c m_{q_1} + 60e_{q_1} m_{q_1} + 832e_{q_2} m_{q_1} - 934e_c m_c - 24e_{q_1} m_c + 624e_{q_2} m_c \right) I[0, 3] \right) \\
& + \frac{C_1 C_3}{2^{21} \times 3^7 \times 5 \times \pi^5} \left( -3m_0^2 \left( 33(e_c + e_{q_1}) m_{q_1} + 34e_c m_c + 22e_{q_1} m_c \right) I[0, 2] - 2 \left( 271e_c m_{q_1} - 268e_{q_1} m_{q_1} \right. \right. \\
& \left. \left. + 26e_c m_c + 12e_{q_1} m_c \right) I[0, 3] \right) \\
& + \frac{C_2^2 e_c}{2^{15} \times 3^5 \times 5 \times \pi^3} \left( 55m_0^2 m_{q_1} m_c I[0, 2] + 12m_{q_1} m_c I[0, 3] + 9[0, 4] \right) \\
& + \frac{C_1 e_c}{2^{26} \times 3^7 \times 5^2 \times \pi^7} \left( (15(531e_c + 175e_{q_1} - 215e_{q_2}) m_{q_1} m_c I[0, 4] + (57e_c - 1316e_{q_1} - 496e_{q_2}) I[0, 5]) \right) \\
& + \frac{e_c}{2^{21} \times 3^5 \times 5^2 \times \pi^5} \left( 15m_0^2 \left( 9(7C_2 + 8C_3) m_{q_1} - 19(2C_2 + C_3) m_c \right) I[0, 4] + 4 \left( -27(C_2 + 7C_3) m_{q_1} \right. \right. \\
& \left. \left. + 28(2C_2 + C_3) m_c \right) I[0, 5] \right), \\
F_2(M^2, s_0) = & \frac{e_c m_c}{2^{22} \times 3^5 \times 7^2 \times \pi^7} \left( 82880 m_{q_1} m_c I[0, 6] - 18063 I[0, 7] \right) \\
& + \frac{C_1 C_2 C_3 m_c}{2^{17} \times 3^6 \times 5 \times \pi^3} \left( 15e_c m_{q_1} m_c I[0, 1] - 7e_c I[0, 2] + 7e_{q_1} I[0, 2] + 4(2e_c - 5e_{q_1}) I[1, 1] \right) \\
& + \frac{C_1 C_2^2 m_c}{2^{16} \times 3^6 \times \pi^3} \left( 18e_c m_{q_1} m_c I[0, 1] - 36e_{q_2} m_{q_1} m_c I[0, 1] - e_c I[0, 2] + 10e_{q_2} I[0, 2] + 2(e_c - 10e_{q_2}) I[1, 1] \right) \\
& + \frac{C_1 C_2 m_c}{2^{21} \times 3^5 \times 5 \times \pi^5} \left( -5e_{q_1} \left( 4(8m_{q_2} - 11m_c) I[0, 3] + 15m_0^2 \left( (8m_{q_2} - 3m_c) I[0, 2] + 4(-2m_{q_2} + 3m_c) \right. \right. \right. \\
& \times I[1, 1] \left. \left. \right) + 12(11m_{q_2} - 20m_c) I[1, 2] \right) + e_c \left( (-1259m_{q_2} + 640m_c) I[0, 3] + 15m_0^2 \left( (65m_{q_2} - 84m_c) I[0, 2] \right. \right. \\
& - 8(m_{q_2} - 18m_c) I[1, 1] + 360(m_{q_2} - 5m_c) I[1, 2] \left. \left. \right) + e_{q_2} \left( 4(114m_{q_2} + 145m_c) I[0, 3] + 15m_0^2 \left( (20m_{q_2} \right. \right. \right. \\
& \left. \left. + 51m_c) I[0, 2] - 8(10m_{q_2} + 21m_c) I[1, 1] + 24(59m_{q_2} + 95m_c) I[1, 2] \right) \right)
\end{aligned}$$



$$\begin{aligned}
& + \frac{C_1 C_3 m_c}{2^{20} \times 3^7 \times \pi^5} \left( e_{q_1} \left( 8(8m_{q_1} - m_c)I[0, 3] + 9m_0^2((7m_{q_1} + 4m_c)I[0, 2] - 4(5m_{q_1} + m_c)I[1, 1]) + 48(5m_{q_1} \right. \right. \\
& + m_c)I[1, 2]) - e_c \left( 59(2m_{q_1} - m_c)I[0, 3] + 9m_0^2((7m_{q_1} + 13m_c)I[0, 2] - 4(2m_{q_1} + 3m_c)I[1, 1]) + 6(16m_{q_1} \right. \\
& + 15m_c)I[1, 2]) \left. \right) \\
& - \frac{C_2^2 e_c m_c}{2^{14} \times 3^5 \times 5 \times \pi^3} \left( 75m_0^2 m_{q_1} m_c I[0, 2] + 20m_{q_1} m_c I[0, 3] + 9I[0, 4] \right) \\
& + \frac{C_1 e_c m_c}{2^{28} \times 3^6 \times 5^2 \times \pi^7} \left( -160(53e_{q_1} + 107e_{q_2})m_{q_1} m_c I[0, 4] + 6537e_c I[0, 5] - 8(77e_{q_1} + 52e_{q_2})I[0, 5] \right. \\
& - 1280(20e_{q_1} + 29e_{q_2})m_{q_1} m_c I[1, 3] + 320e_c m_{q_1} m_c (-31I[0, 4] + 84I[1, 3]) + 180(9e_c + 29e_{q_1} + 4e_{q_2})I[1, 4] \left. \right) \\
& + \frac{e_c m_c}{2^{20} \times 3^4 \times 5^2 \times \pi^5} \left( 120m_0^2(-3(C_2 + C_3)m_{q_1} + (2C_2 + C_3)m_c)I[0, 4] + (9(5C_2 + 32C_3)m_{q_1} - 46(2C_2 \right. \\
& + C_3)m_c)I[0, 5] \left. \right), \tag{25}
\end{aligned}$$

where  $C_1 = \langle g_s^2 G^2 \rangle$  is gluon condensate;  $C_2 = \langle \bar{q}_1 q_1 \rangle$  and  $C_3 = \langle \bar{q}_2 q_2 \rangle$  are corresponding light-quark condensates. The function  $I[n, m]$  is given as

$$I[n, m] = \int_{\mathcal{M}}^{s_0} ds e^{-s/M^2} s^n (s - \mathcal{M})^m, \tag{26}$$

where  $\mathcal{M} = 4m_c^2$  for the  $P_c(4457)$  and  $[dd][uc]\bar{c}$  states;  $\mathcal{M} = (2m_c + m_s)^2$  for the  $[uu][sc]\bar{c}$  and  $[dd][sc]\bar{c}$  states; and,  $\mathcal{M} = (2m_c + 2m_s)^2$  for the  $[ss][uc]\bar{c}$  and  $[ss][dc]\bar{c}$  states.

- 
- [1] R. Aaij, et al., Observation of  $J/\psi p$  Resonances Consistent with Pentaquark States in  $\Lambda_b^0 \rightarrow J/\psi K^- p$  Decays, Phys. Rev. Lett. 115 (2015) 072001. [arXiv:1507.03414](#), [doi:10.1103/PhysRevLett.115.072001](#).
- [2] R. Aaij, et al., Observation of a narrow pentaquark state,  $P_c(4312)^+$ , and of two-peak structure of the  $P_c(4450)^+$ , Phys. Rev. Lett. 122 (22) (2019) 222001. [arXiv:1904.03947](#), [doi:10.1103/PhysRevLett.122.222001](#).
- [3] R. Aaij, et al., Evidence of a  $J/\psi\Lambda$  structure and observation of excited  $\Xi^-$  states in the  $\Xi_b^- \rightarrow J/\psi\Lambda K^-$  decay, Sci. Bull. 66 (2021) 1278–1287. [arXiv:2012.10380](#), [doi:10.1016/j.scib.2021.02.030](#).
- [4] R. Aaij, et al., Observation of a  $J/\psi\Lambda$  Resonance Consistent with a Strange Pentaquark Candidate in  $B \rightarrow J/\psi\Lambda p^-$  Decays, Phys. Rev. Lett. 131 (3) (2023) 031901. [arXiv:2210.10346](#), [doi:10.1103/PhysRevLett.131.031901](#).
- [5] A. Hayrapetyan, et al., Observation of the  $\Lambda_b^0 \rightarrow J/\psi\Xi^- K^+$  decay (1 2024). [arXiv:2401.16303](#).
- [6] A. Esposito, A. L. Guerrieri, F. Piccinini, A. Pilloni, A. D. Polosa, Four-Quark Hadrons: an Updated Review, Int. J. Mod. Phys. A 30 (2015) 1530002. [arXiv:1411.5997](#), [doi:10.1142/S0217751X15300021](#).
- [7] A. Esposito, A. Pilloni, A. D. Polosa, Multiquark Resonances, Phys. Rept. 668 (2017) 1–97. [arXiv:1611.07920](#), [doi:10.1016/j.physrep.2016.11.002](#).
- [8] S. L. Olsen, T. Skwarnicki, D. Zieminska, Nonstandard heavy mesons and baryons: Experimental evidence, Rev. Mod. Phys. 90 (1) (2018) 015003. [arXiv:1708.04012](#), [doi:10.1103/RevModPhys.90.015003](#).
- [9] R. F. Lebed, R. E. Mitchell, E. S. Swanson, Heavy-Quark QCD Exotica, Prog. Part. Nucl. Phys. 93 (2017) 143–194. [arXiv:1610.04528](#), [doi:10.1016/j.pnpnp.2016.11.003](#).
- [10] M. Nielsen, F. S. Navarra, S. H. Lee, New Charmonium States in QCD Sum Rules: A Concise Review, Phys. Rept. 497 (2010) 41–83. [arXiv:0911.1958](#), [doi:10.1016/j.physrep.2010.07.005](#).
- [11] N. Brambilla, S. Eidelman, C. Hanhart, A. Nefediev, C.-P. Shen, C. E. Thomas, A. Vairo, C.-Z. Yuan, The XYZ states: experimental and theoretical status and perspectives, Phys. Rept. 873 (2020) 1–154. [arXiv:1907.07583](#), [doi:10.1016/j.physrep.2020.05.001](#).
- [12] S. Agaev, K. Azizi, H. Sundu, Four-quark exotic mesons, Turk. J. Phys. 44 (2) (2020) 95–173. [arXiv:2004.12079](#), [doi:10.3906/fiz-2003-15](#).
- [13] H.-X. Chen, W. Chen, X. Liu, S.-L. Zhu, The hidden-charm pentaquark and tetraquark states, Phys. Rept. 639 (2016) 1–121. [arXiv:1601.02092](#), [doi:10.1016/j.physrep.2016.05.004](#).

- [14] A. Ali, J. S. Lange, S. Stone, Exotics: Heavy Pentaquarks and Tetraquarks, *Prog. Part. Nucl. Phys.* 97 (2017) 123–198. [arXiv:1706.00610](#), [doi:10.1016/j.pnpnp.2017.08.003](#).
- [15] F.-K. Guo, C. Hanhart, U.-G. Meißner, Q. Wang, Q. Zhao, B.-S. Zou, Hadronic molecules, *Rev. Mod. Phys.* 90 (1) (2018) 015004, [Erratum: *Rev. Mod. Phys.* 94, 029901 (2022)]. [arXiv:1705.00141](#), [doi:10.1103/RevModPhys.90.015004](#).
- [16] Y.-R. Liu, H.-X. Chen, W. Chen, X. Liu, S.-L. Zhu, Pentaquark and Tetraquark states, *Prog. Part. Nucl. Phys.* 107 (2019) 237–320. [arXiv:1903.11976](#), [doi:10.1016/j.pnpnp.2019.04.003](#).
- [17] G. Yang, J. Ping, J. Segovia, Tetra- and penta-quark structures in the constituent quark model, *Symmetry* 12 (11) (2020) 1869. [arXiv:2009.00238](#), [doi:10.3390/sym12111869](#).
- [18] X.-K. Dong, F.-K. Guo, B.-S. Zou, A survey of heavy-antiheavy hadronic molecules, *Progr. Phys.* 41 (2021) 65–93. [arXiv:2101.01021](#), [doi:10.13725/j.cnki.pip.2021.02.001](#).
- [19] X.-K. Dong, F.-K. Guo, B.-S. Zou, A survey of heavy-heavy hadronic molecules, *Commun. Theor. Phys.* 73 (12) (2021) 125201. [arXiv:2108.02673](#), [doi:10.1088/1572-9494/ac27a2](#).
- [20] H.-X. Chen, W. Chen, X. Liu, Y.-R. Liu, S.-L. Zhu, An updated review of the new hadron states, *Rept. Prog. Phys.* 86 (2) (2023) 026201. [arXiv:2204.02649](#), [doi:10.1088/1361-6633/aca3b6](#).
- [21] L. Meng, B. Wang, G.-J. Wang, S.-L. Zhu, Chiral perturbation theory for heavy hadrons and chiral effective field theory for heavy hadronic molecules, *Phys. Rept.* 1019 (2023) 1–149. [arXiv:2204.08716](#), [doi:10.1016/j.physrep.2023.04.003](#).
- [22] G.-J. Wang, R. Chen, L. Ma, X. Liu, S.-L. Zhu, Magnetic moments of the hidden-charm pentaquark states, *Phys. Rev. D* 94 (9) (2016) 094018. [arXiv:1605.01337](#), [doi:10.1103/PhysRevD.94.094018](#).
- [23] U. Özdem, K. Azizi, Electromagnetic multipole moments of the  $P_c^+$  (4380) pentaquark in light-cone QCD, *Eur. Phys. J. C* 78 (5) (2018) 379. [arXiv:1803.06831](#), [doi:10.1140/epjc/s10052-018-5873-2](#).
- [24] E. Ortiz-Pacheco, R. Bijker, C. Fernández-Ramírez, Hidden charm pentaquarks: mass spectrum, magnetic moments, and photocouplings, *J. Phys. G* 46 (6) (2019) 065104. [arXiv:1808.10512](#), [doi:10.1088/1361-6471/ab096d](#).
- [25] Y.-J. Xu, Y.-L. Liu, M.-Q. Huang, The magnetic moment of  $P_c(4312)$  as a  $\bar{D}\Sigma_c$  molecular state, *Eur. Phys. J. C* 81 (5) (2021) 421. [arXiv:2008.07937](#), [doi:10.1140/epjc/s10052-021-09211-8](#).
- [26] U. Özdem, Electromagnetic properties of the  $P_c(4312)$  pentaquark state, *Chin. Phys. C* 45 (2) (2021) 023119. [doi:10.1088/1674-1137/abd01c](#).
- [27] U. Özdem, Magnetic dipole moments of the hidden-charm pentaquark states:  $P_c(4440)$ ,  $P_c(4457)$  and  $P_{cs}(4459)$ , *Eur. Phys. J. C* 81 (4) (2021) 277. [arXiv:2102.01996](#), [doi:10.1140/epjc/s10052-021-09070-3](#).
- [28] M.-W. Li, Z.-W. Liu, Z.-F. Sun, R. Chen, Magnetic moments and transition magnetic moments of Pc and Pcs states, *Phys. Rev. D* 104 (5) (2021) 054016. [arXiv:2106.15053](#), [doi:10.1103/PhysRevD.104.054016](#).
- [29] U. Özdem, Electromagnetic properties of  $D^-(*)\Xi c'$ ,  $D^-(*)\Lambda c$ ,  $D^-s(*)\Lambda c$  and  $D^-s(*)\Xi c$  pentaquarks, *Phys. Lett. B* 846 (2023) 138267. [arXiv:2303.10649](#), [doi:10.1016/j.physletb.2023.138267](#).
- [30] F.-L. Wang, X. Liu, Higher molecular  $P\psi s\Lambda/\Sigma$  pentaquarks arising from the  $\Xi c(^*,*)D^{-1}/\Xi c(^*,*)D^{-2*}$  interactions, *Phys. Rev. D* 108 (5) (2023) 054028. [arXiv:2307.08276](#), [doi:10.1103/PhysRevD.108.054028](#).
- [31] U. Özdem, Investigation of magnetic moment of Pcs(4338) and Pcs(4459) pentaquark states, *Phys. Lett. B* 836 (2023) 137635. [arXiv:2208.07684](#), [doi:10.1016/j.physletb.2022.137635](#).
- [32] F. Gao, H.-S. Li, Magnetic moments of hidden-charm strange pentaquark states\*, *Chin. Phys. C* 46 (12) (2022) 123111. [arXiv:2112.01823](#), [doi:10.1088/1674-1137/ac8651](#).
- [33] F. Guo, H.-S. Li, Analysis of the hidden-charm pentaquark states based on magnetic moment and transition magnetic moment, *Eur. Phys. J. C* 84 (4) (2024) 392. [arXiv:2304.10981](#), [doi:10.1140/epjc/s10052-024-12699-5](#).
- [34] U. Özdem, Magnetic moments of pentaquark states in light-cone sum rules, *Eur. Phys. J. A* 58 (3) (2022) 46. [doi:10.1140/epja/s10050-022-00700-2](#).
- [35] F.-L. Wang, S.-Q. Luo, H.-Y. Zhou, Z.-W. Liu, X. Liu, Exploring the electromagnetic properties of the  $\Xi c(^*,*)D^-s^*$  and  $\Omega c(^*)D^-s^*$  molecular states, *Phys. Rev. D* 108 (3) (2023) 034006. [arXiv:2210.02809](#), [doi:10.1103/PhysRevD.108.034006](#).
- [36] F.-L. Wang, H.-Y. Zhou, Z.-W. Liu, X. Liu, What can we learn from the electromagnetic properties of hidden-charm molecular pentaquarks with single strangeness?, *Phys. Rev. D* 106 (5) (2022) 054020. [arXiv:2208.10756](#), [doi:10.1103/PhysRevD.106.054020](#).
- [37] U. Özdem, Analysis of the isospin eigenstate  $\bar{D}\Sigma_c$ ,  $\bar{D}^*\Sigma_c$ , and  $\bar{D}\Sigma_c^*$  pentaquarks by their electromagnetic properties, *Eur. Phys. J. C* 84 (8) (2024) 769. [arXiv:2401.12678](#), [doi:10.1140/epjc/s10052-024-13124-7](#).
- [38] H.-S. Li, F. Guo, Y.-D. Lei, F. Gao, Magnetic moments and axial charges of the octet hidden-charm molecular pentaquark family, *Phys. Rev. D* 109 (9) (2024) 094027. [arXiv:2401.14767](#), [doi:10.1103/PhysRevD.109.094027](#).
- [39] H.-S. Li, Molecular pentaquark magnetic moments in heavy pentaquark chiral perturbation theory, *Phys. Rev. D* 109 (11) (2024) 114039. [arXiv:2401.14759](#), [doi:10.1103/PhysRevD.109.114039](#).
- [40] U. Özdem, Investigation on the electromagnetic properties of the  $D^{(*)}\Sigma_c^{(*)}$  molecules (5 2024). [arXiv:2405.07273](#).
- [41] U. Özdem, Elucidating the nature of hidden-charm pentaquark states with spin-3/2 through their electromagnetic form factors, *Phys. Lett. B* 851 (2024) 138551. [arXiv:2402.03802](#), [doi:10.1016/j.physletb.2024.138551](#).
- [42] H. Mutuk, X.-W. Kang, Unveiling the structure of hidden-bottom strange pentaquarks via magnetic moments, *Phys. Lett. B* 855 (2024) 138772. [arXiv:2405.07066](#), [doi:10.1016/j.physletb.2024.138772](#).
- [43] H. Mutuk, Magnetic moments of hidden-bottom pentaquark states, *Eur. Phys. J. C* 84 (8) (2024) 874. [arXiv:2403.16616](#), [doi:10.1140/epjc/s10052-024-13263-x](#).
- [44] V. Pascalutsa, M. Vanderhaeghen, Magnetic moment of the Delta(1232)-resonance in chiral effective field theory, *Phys. Rev. Lett.* 94 (2005) 102003. [arXiv:nucl-th/0412113](#), [doi:10.1103/PhysRevLett.94.102003](#).
- [45] V. Pascalutsa, M. Vanderhaeghen, Chiral effective-field theory in the Delta(1232) region: I. Pion electroproduction on the

- nucleon, Phys. Rev. D 73 (2006) 034003. [arXiv:hep-ph/0512244](#), [doi:10.1103/PhysRevD.73.034003](#).
- [46] V. Pascalutsa, M. Vanderhaeghen, Chiral effective-field theory in the Delta(1232) region. II. Radiative pion photoproduction, Phys. Rev. D 77 (2008) 014027. [arXiv:0709.4583](#), [doi:10.1103/PhysRevD.77.014027](#).
- [47] K. U. Can, G. Erkol, B. Isildak, M. Oka, T. T. Takahashi, Electromagnetic properties of doubly charmed baryons in Lattice QCD, Phys. Lett. B 726 (2013) 703–709. [arXiv:1306.0731](#), [doi:10.1016/j.physletb.2013.09.024](#).
- [48] K. U. Can, G. Erkol, B. Isildak, M. Oka, T. T. Takahashi, Electromagnetic structure of charmed baryons in Lattice QCD, JHEP 05 (2014) 125. [arXiv:1310.5915](#), [doi:10.1007/JHEP05\(2014\)125](#).
- [49] V. L. Chernyak, I. R. Zhitnitsky, B meson exclusive decays into baryons, Nucl. Phys. B 345 (1990) 137–172. [doi:10.1016/0550-3213\(90\)90612-H](#).
- [50] V. M. Braun, I. E. Filyanov, QCD Sum Rules in Exclusive Kinematics and Pion Wave Function, Z. Phys. C 44 (1989) 157. [doi:10.1007/BF01548594](#).
- [51] I. I. Balitsky, V. M. Braun, A. V. Kolesnichenko, Radiative Decay  $\Sigma^+ \rightarrow p \gamma$  in Quantum Chromodynamics, Nucl. Phys. B 312 (1989) 509–550. [doi:10.1016/0550-3213\(89\)90570-1](#).
- [52] V. M. Belyaev, B. L. Ioffe, Determination of the baryon mass and baryon resonances from the quantum-chromodynamics sum rule. Strange baryons, Sov. Phys. JETP 57 (1983) 716–721.
- [53] H. J. Weber, H. Arenhovel, Isobar Configurations in Nuclei, Phys. Rept. 36 (1978) 277–348. [doi:10.1016/0370-1573\(78\)90187-4](#).
- [54] S. Nozawa, D. B. Leinweber, Electromagnetic form-factors of spin 3/2 baryons, Phys. Rev. D 42 (1990) 3567–3571. [doi:10.1103/PhysRevD.42.3567](#).
- [55] V. Pascalutsa, M. Vanderhaeghen, S. N. Yang, Electromagnetic excitation of the Delta(1232)-resonance, Phys. Rept. 437 (2007) 125–232. [arXiv:hep-ph/0609004](#), [doi:10.1016/j.physrep.2006.09.006](#).
- [56] G. Ramalho, M. T. Pena, F. Gross, Electric quadrupole and magnetic octupole moments of the Delta, Phys. Lett. B 678 (2009) 355–358. [arXiv:0902.4212](#), [doi:10.1016/j.physletb.2009.06.052](#).
- [57] K.-C. Yang, W. Y. P. Hwang, E. M. Henley, L. S. Kisslinger, QCD sum rules and neutron proton mass difference, Phys. Rev. D 47 (1993) 3001–3012. [doi:10.1103/PhysRevD.47.3001](#).
- [58] V. M. Belyaev, B. Y. Blok, CHARMED BARYONS IN QUANTUM CHROMODYNAMICS, Z. Phys. C 30 (1986) 151. [doi:10.1007/BF01560689](#).
- [59] P. Ball, V. M. Braun, N. Kivel, Photon distribution amplitudes in QCD, Nucl. Phys. B 649 (2003) 263–296. [arXiv:hep-ph/0207307](#), [doi:10.1016/S0550-3213\(02\)01017-9](#).
- [60] U. Özdem, Electromagnetic properties of doubly heavy pentaquark states, Eur. Phys. J. Plus 137 (2022) 936. [arXiv:2201.00979](#), [doi:10.1140/epjp/s13360-022-03125-4](#).
- [61] U. Özdem, Electromagnetic form factors of the Bc-like tetraquarks: Molecular and diquark-antidiquark pictures, Phys. Lett. B 838 (2023) 137750. [arXiv:2211.10169](#), [doi:10.1016/j.physletb.2023.137750](#).
- [62] R. L. Workman, et al., Review of Particle Physics, PTEP 2022 (2022) 083C01. [doi:10.1093/ptep/ptac097](#).
- [63] R. Aaij, et al., Observation of a narrow pentaquark state,  $P_c(4312)^+$ , and of two-peak structure of the  $P_c(4450)^+$ , Phys. Rev. Lett. 122 (22) (2019) 222001. [arXiv:1904.03947](#), [doi:10.1103/PhysRevLett.122.222001](#).
- [64] Z.-G. Wang, Analysis of the  $P_c(4312)$ ,  $P_c(4440)$ ,  $P_c(4457)$  and related hidden-charm pentaquark states with QCD sum rules, Int. J. Mod. Phys. A 35 (01) (2020) 2050003. [arXiv:1905.02892](#), [doi:10.1142/S0217751X20500037](#).
- [65] Z.-G. Wang, Analysis of the  $\frac{3}{2}^\pm$  pentaquark states in the diquark-diquark-antiquark model with QCD sum rules, Nucl. Phys. B 913 (2016) 163–208. [arXiv:1512.04763](#), [doi:10.1016/j.nuclphysb.2016.09.009](#).
- [66] B. L. Ioffe, QCD at low energies, Prog. Part. Nucl. Phys. 56 (2006) 232–277. [arXiv:hep-ph/0502148](#), [doi:10.1016/j.pnpnp.2005.05.001](#).
- [67] S. Narison,  $\overline{m}_{c,b}$ ,  $\langle \alpha_s G^2 \rangle$  and  $\alpha_s$  from Heavy Quarkonia, Nucl. Part. Phys. Proc. 300-302 (2018) 153–164. [doi:10.1016/j.nuclphysbps.2018.12.026](#).